

# VERIFICATION OF BLAST DEMOLITION PROBLEMS USING NUMERICAL AND EXPERIMENTAL APPROACHES

Daigoro Isobe<sup>1</sup>, Masashi Eguchi<sup>2</sup>, Kensuke Imanishi<sup>2</sup> and Zion Sasaki<sup>2</sup>

## ABSTRACT

One of the objectives of this study is to perform some blast demolition analyses of framed structures using a dynamic finite element code, whose validity against impact collapse problems of full-model large-scale structures has recently been developed and verified. Another objective of this study is to develop a mimic demolition experimental system that uses magnetic devices to express member fracture caused by explosion. The magnetic field of the devices is controlled by a blast interval controller and power switches, which control the binding of each connection in the framed structure. The experimental system does not use explosives or any such dangerous substances, and multicycle use is possible. Some experiments are carried out for comparison with the numerical results.

## KEY WORDS

blast demolition, framed structures, ASI-Gauss technique, finite element analysis, demolition experiment.

## INTRODUCTION

The technology used in the demolition of old worn-out buildings has always been of major interest and challenge in civil engineering. Because conventional demolition techniques using a hydraulic concrete crusher, a concrete cutter or a nonexplosive demolition agent are lengthy and costly to meet the heavy demand for demolition work, a controlled explosion technique using high explosives has been developed in recent years. Although the blast demolition technique increases work efficiency, it poses a high risk of damaging neighboring buildings, especially in urban areas (Williams 1990). It also requires high levels of knowledge and experience (e.g., Yarimar 1989, Kinoshita et al. 1989), which are very difficult for general engineers to master. Although there are some representative demolition companies in USA and Europe, the blast demolition technique has been only used in a few cases in Japan; this may or may not be due to the above reasons. To familiarize the demolition technique among construction companies, numerical assumptions using computational analysis in devising the blast demolition have become essential in ensuring the success of this technique.

---

<sup>1</sup> Associate Professor, Department of Eng. Mech. and Energy, Univ. of Tsukuba, 1-1-1 Tennodai, Tsukuba-shi, Ibaraki 305-8573, Japan, Phone +81-29-853-6191, FAX +81-29-853-5207, isobe@kz.tsukuba.ac.jp

<sup>2</sup> Graduate student, Univ. of Tsukuba, 1-1-1 Tennodai, Tsukuba-shi, Ibaraki 305-8573, Japan, Phone +81-29-853-5461, FAX +81-29-853-5207, [e011264], [e011258], [z\_sasaki]@edu.esys.tsukuba.ac.jp

Thus far, there are few numerical examples showing a high performance in dealing with structurally discontinuous problems, such as the Distinct Element Method (DEM) (Cundall 1971) or the Discontinuous Deformation Analysis (DDA) (Shi and Goodman 1984), applied to demolition or seismic damage analyses (e.g., Tosaka et al. 1988, Ma et al. 1995). Although these examples have shown the collapse phenomenon, there are no adequate numerical procedures to track the demolition process that includes coupled and complicated failure mechanisms.

The first objective of this study is to perform some blast demolition analyses using a dynamic finite element code, whose validity against impact collapse problems of full-model large-scale structures has recently been developed and verified (Isobe and Lynn 2004). The code is based on the ASI-Gauss technique, a modified version of the formerly developed Adaptively Shifted Integration (ASI) technique (Toi and Isobe 1993, Isobe and Toi 2000) for the linear Timoshenko beam element, which computes highly accurate elastoplastic solutions even with the minimum number of elements per member. The ASI-Gauss technique gains still a higher accuracy particularly in the elastic range, by placing the numerical integration points of the two consecutive elements forming an elastically deformed member in such a way that stresses and strains are evaluated at the Gaussian integration points of the two-element member. Moreover, the technique can be used to express member fracture, by shifting the numerical integration point to an appropriate position and by releasing the resultant forces in the element simultaneously. Some blast demolition analyses are performed on framed structures, where the blast conditions are changed to see the difference in the demolition modes.

We also developed a mimic demolition experimental system that uses magnetic devices to express member fracture caused by explosion. Two electromagnetic devices are mounted on both sides of an aluminum pipe, and the pipes are connected via a steel-made connection with a magnetic field. The magnetic field is controlled by a blast interval controller and power switches, which control the binding of each connection in the framed structure. The experimental system does not use explosives or any such dangerous substances, and multicycle use is possible. Some experiments are carried out for comparison with the numerical results.

## **NUMERICAL METHODS**

In the ASI technique, the numerical integration point is shifted immediately after the formation of a fully plastic section in an element to form a plastic hinge exactly at that section. As a result, the ASI technique gives a converged solution with a small number of elements per member and consequently reduces the calculation cost to some extent. However, the solution in the elastic range is not accurate when the number of elements per member is very small, due to the one-point integration used in the element for avoiding shear locking. Thus the technique is modified into an ASI-Gauss technique to improve the accuracy in the elastic range. In this section, general information on both schemes is described.

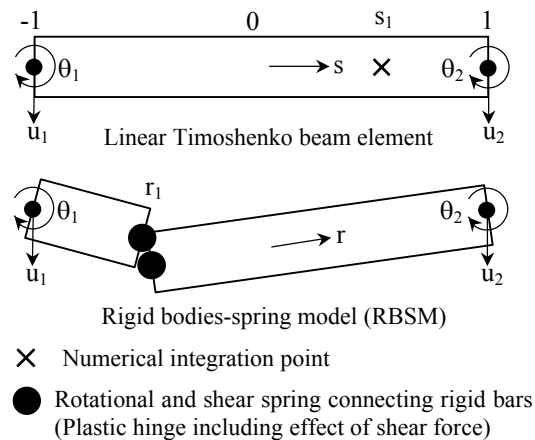


Figure 1: Linear Timoshenko beam element and its physical equivalent

### ASI AND ASI-GAUSS TECHNIQUES

Figure 1 shows a linear Timoshenko beam element and its physical equivalence to the rigid bodies-spring model (RBSM). As shown in the figure, the relationship between the locations of the numerical integration point and the stress evaluation point where a plastic hinge is actually formed is expressed (Toi and Isobe 1993) as

$$r = -s. \quad (1)$$

In the above equation,  $s$  is the location of the numerical integration point and  $r$  the location where stresses and strains are actually evaluated. We refer to  $r$  as the stress evaluation point later in this section.  $s$  is a nondimensional quantity, which is defined as  $z/(L/2)$ , where  $L$  is the length of the element.  $s$  takes a value between -1 and 1.

In both the ASI and ASI-Gauss techniques, the numerical integration point is shifted adaptively when a fully plastic section is formed within an element to form a plastic hinge exactly at that section. When the plastic hinge is determined to be unloaded, the corresponding numerical integration point is shifted back to its normal position. Here, the normal position means the location where the numerical integration point is placed when the element acts elastically. By doing so, the plastic behavior of the element is simulated appropriately, and the converged solution is achieved with only a small number of elements per member. However, in the ASI technique, the numerical integration point is placed at the midpoint of the linear Timoshenko beam element, which is considered to be optimal for one-point integration, when the entire region of the element behaves elastically. When the number of elements per member is very small, solutions in the elastic range are not accurate since one-point integration is used to evaluate the low-degree displacement function of the beam element.

The main difference between the ASI and ASI-Gauss techniques lies in the normal position of the numerical integration point. In the ASI-Gauss technique, two consecutive elements forming a member are considered as a subset, and the numerical integration points of an elastically deformed member are placed such that the stress evaluation points coincide

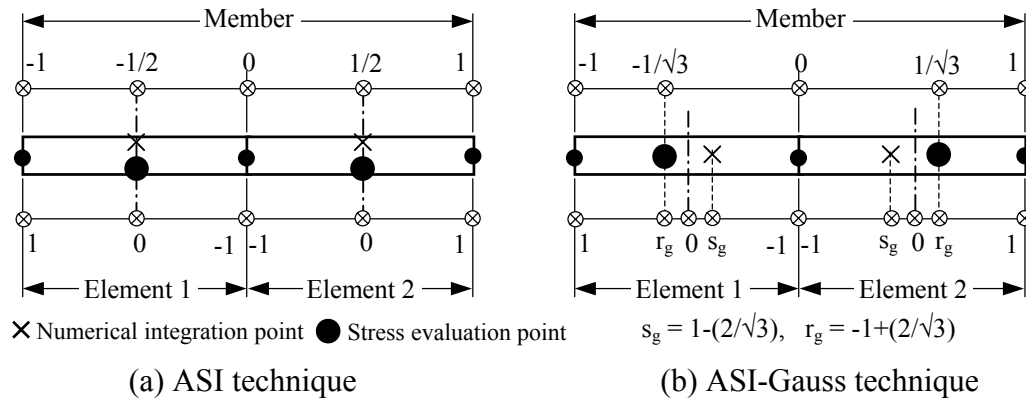


Figure 2: Locations of numerical integration and stress evaluation points in elastic range

with the Gaussian integration points of the member. This means that stresses and strains are evaluated at the Gaussian integration points of elastically deformed members. Gaussian integration points are optimal for two-point integration and the accuracy of bending deformation is mathematically guaranteed. In this way, the ASI-Gauss technique takes advantage of two-point integration while using one-point integration in actual calculations.

Figure 2 shows the locations of the numerical integrations points of elastically deformed elements in the ASI and ASI-Gauss techniques. The elemental stiffness matrix, generalized strain and resultant force increment vectors for the ASI technique are given by Eqs. (2a) ~ (2c) and those for the ASI-Gauss technique by Eqs. (3a) ~ (3c).

$$[K] = L[B(0)]^T [D(0)][B(0)] \quad (2a)$$

$$\{\Delta\varepsilon(0)\} = [B(0)]\{\Delta u\} \quad (2b)$$

$$\{\Delta\sigma(0)\} = [D(0)]\{\Delta\varepsilon(0)\} \quad (2c)$$

$$[K] = L[B(1 - 2/\sqrt{3})]^T [D(-1 + 2/\sqrt{3})][B(1 - 2/\sqrt{3})] \quad (3a)$$

$$\{\Delta\varepsilon(-1 + 2/\sqrt{3})\} = [B(1 - 2/\sqrt{3})]\{\Delta u\} \quad (3b)$$

$$\{\Delta\sigma(-1 + 2/\sqrt{3})\} = [D(-1 + 2/\sqrt{3})]\{\Delta\varepsilon(-1 + 2/\sqrt{3})\} \quad (3c)$$

Here,  $\{\Delta\varepsilon\}$ ,  $\{\Delta\sigma\}$  and  $\{\Delta u\}$  are the generalized strain increment vector, generalized stress (resultant force) increment vector and nodal displacement increment vector, respectively.  $\Delta$  denotes the increment.

The plastic potential used in this study is expressed by

$$f \equiv \left(\frac{M_x}{M_{x0}}\right)^2 + \left(\frac{M_y}{M_{y0}}\right)^2 + \left(\frac{N}{N_0}\right)^2 + \left(\frac{M_z}{M_{z0}}\right)^2 - 1 = f_y - 1 = 0. \quad (4)$$

Here,  $f_y$  is the yield function, and  $M_x$ ,  $M_y$ ,  $N$  and  $M_z$  are the bending moments around the x- and y- axes, axial force and torsional moment, respectively. Those with the subscript 0 are

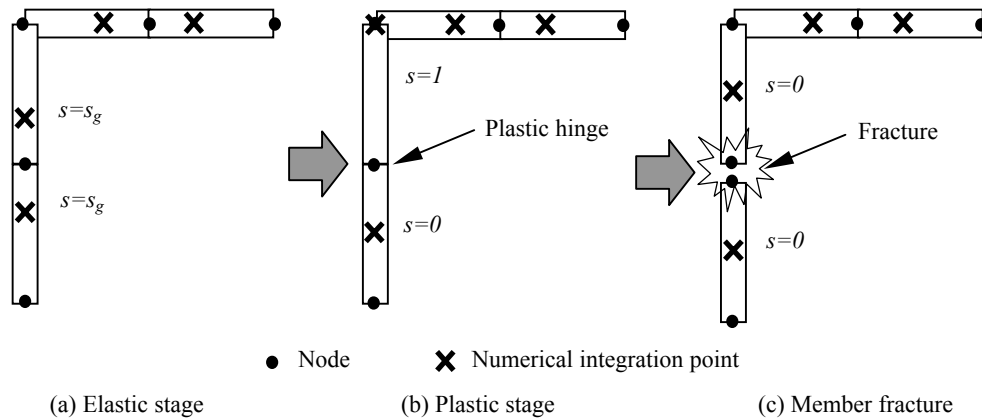


Figure 3: Locations of numerical integration points in ASI-Gauss technique

values that result in a fully plastic section in an element when they act on a cross section independently. The effect of shear force is neglected in the yield function. In this study, we use a consistent mass matrix, which is assumed to be unaffected by the shifting of numerical integration points. Newmark's  $\beta$  method is used as a time integration scheme and the conjugate gradient (CG) method is used as a solver to reduce the need for memory resources.

#### MEMBER FRACTURE AND ELEMENTAL CONTACT

A plastic hinge is likely to occur before it develops into a member fracture, and the plastic hinge is expressed by shifting the numerical integration point to the opposite end of the fully plastic section. Accordingly, the numerical integration point of the adjacent element forming the same member is shifted back to its midpoint where it is appropriate for one-point integration. Figure 3 shows the locations of numerical integration points for each stage in the ASI-Gauss technique. A member fracture is determined, in this study, by examining axial and bending strains in two elements forming a member, using the following conditions.

$$\left| \frac{\kappa_x}{\kappa_{fx}} \right| - 1 \geq 0, \quad \left| \frac{\kappa_y}{\kappa_{fy}} \right| - 1 \geq 0, \quad \left( \frac{\varepsilon_z}{\varepsilon_{fz}} \right) - 1 \geq 0 \quad (5)$$

Here,  $\kappa_x$ ,  $\kappa_y$ ,  $\varepsilon_z$ ,  $\kappa_{fx}$ ,  $\kappa_{fy}$  and  $\varepsilon_{fz}$  are the bending strains around the x- and y- axes, the axial tension strain and the critical values for each strain, respectively. When fracture is judged to occur, a new node is created at the fractured section and the numerical integration point of the element is shifted back to its midpoint. The resultant forces exerting on the fractured section are released instantly at the next step after fracture has occurred. A blast at a section is expressed by inducing member fracture at the relevant section. The nodal mass is equally redistributed at each separated node after the step.

The contact between the elements is determined using geometrical relations, and is expressed by connecting the corresponding nodes with two types of gap elements; (1) a hinge element with only axial stiffness, used between column elements at blast points, and (2) a beam element with axial and bending stiffnesses, used between other sets of elements.

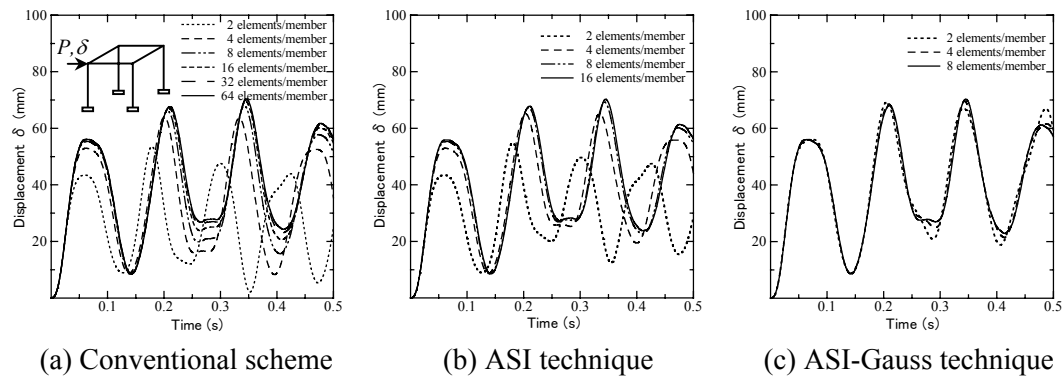


Figure 4: Elastoplastic responses of a space frame

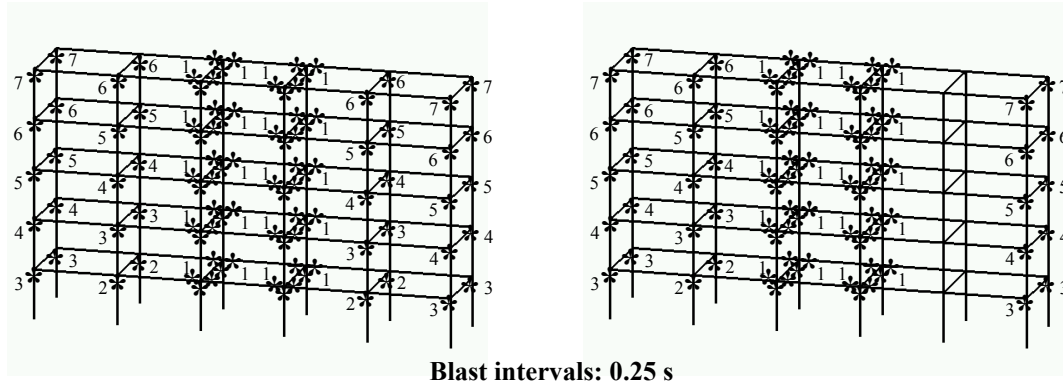
## NUMERICAL EXAMPLES

### Elastoplastic response analysis

An elastoplastic response analysis is performed to evaluate the convergency of the schemes. A load of 12 kN is applied to a space frame as shown in Fig. 4. The conventional scheme shows a very slow convergence and sixteen-element modeling is necessary to obtain the converged solution. Although the ASI technique gives comparatively better results than the conventional scheme, a difference in the vibration mode can be observed in fewer-element modeling. On the other hand, the ASI-Gauss technique shows a very fast convergence and nearly converged solutions are obtained even when the number of elements per member is two. A higher reliability of the ASI-Gauss technique is thus confirmed in structural response analyses.

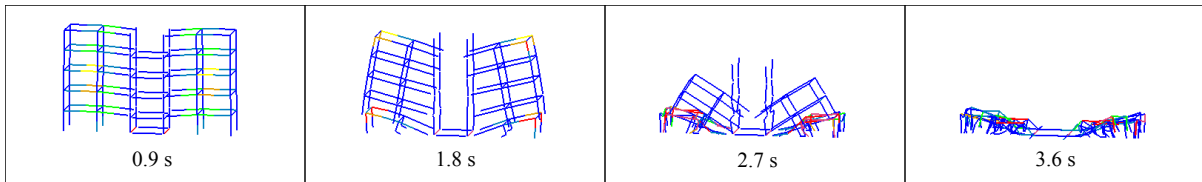
### Blast demolition analyses

The ASI-Gauss technique is applied to the blast demolition analyses of a 5-story framed structure, with different blast sequences as shown in Fig. 5. The main properties of the structure are as follows: each span length 6.0 m (beam), 3.6 m (column), 30 cm\*30 cm H-type beams, 30 cm\*30 cm box-type columns, with Young's modulus of 214 GPa and Poisson's ratio of 0.3 (steel), critical values of bending strains  $3.2 \cdot 10^{-4}$  rad/mm (beam),  $5.3 \cdot 10^{-4}$  rad/mm (column) and tension strain 0.17. The mass of floor slabs and walls is taken into account by summing the corresponding quantities into the densities of each member. The analytical conditions are as follows: time increment 0.1 ms, numerical damping applied (Newmark's  $\beta$  method,  $\beta=4/9$ ), structural damping not considered. The blast sequence of Case 1 is designed to start from the central core towards the outer structure, to accomplish the demolition successfully by collapsing all the structural members inward. The blast sequence in Case 2, however, assumes the case when the explosives in one of the series of columns have completely failed to set off. Inevitably, a difference appears in the demolition modes as shown in Fig. 6. The structure is successfully brought down in 3.6 s with no fragments dispersed around the region in Case 1, while in Case 2, the right-hand side of the structure where the explosives are unsuccessfully installed, stands unstably for a while and slowly topples down to the outer region.

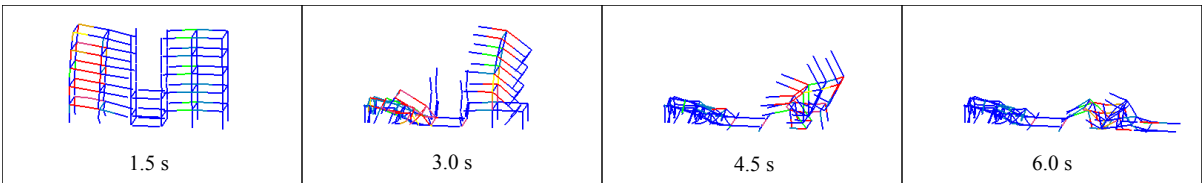


(a) Case 1 (b) Case 2

Figure 5: Blast sequences in demolition analyses



(a) Case 1



(b) Case 2

Figure 6: Difference in demolition modes

## EXPERIMENTS

A mimic demolition experimental system is developed in this study to enable quantitative comparison with numerical analyses. Two electromagnetic devices (KANETEC, KE-4RA, max. attach force = 110 N for beams, KE-4B, max. attach force = 400 N for columns) are mounted on both sides of an aluminum pipe as shown in Fig. 7, and the members are connected via steel connectors with the magnetic field generated by the electromagnetic devices. Power is supplied to these devices through a 4-pin connector jack and a telephone cord. Blast intervals and on/off of the magnetic field are controlled by the blast interval controller and power switches, which are connected to a PC and a power supply. The magnetic field of the device at the blast point is sequentially released by the PC, to express member fracture caused by explosion.

The properties and conditions used for the analysis are as follows: each span length 34 cm (beam), 28 cm (column), 3 cm\*3 cm box-type beams, 4 cm\*4 cm box-type columns, with Young's modulus of 70 GPa and Poisson's ratio of 0.345 (aluminum), critical values of bending strains  $2.4 \cdot 10^{-4}$  rad/mm (beam),  $3.1 \cdot 10^{-4}$  rad/mm (column) and tension strain

$2.7 \cdot 10^{-4}$  (beam),  $3.0 \cdot 10^{-4}$  (column), time increment 0.01 ms, numerical damping applied and structural damping not considered.

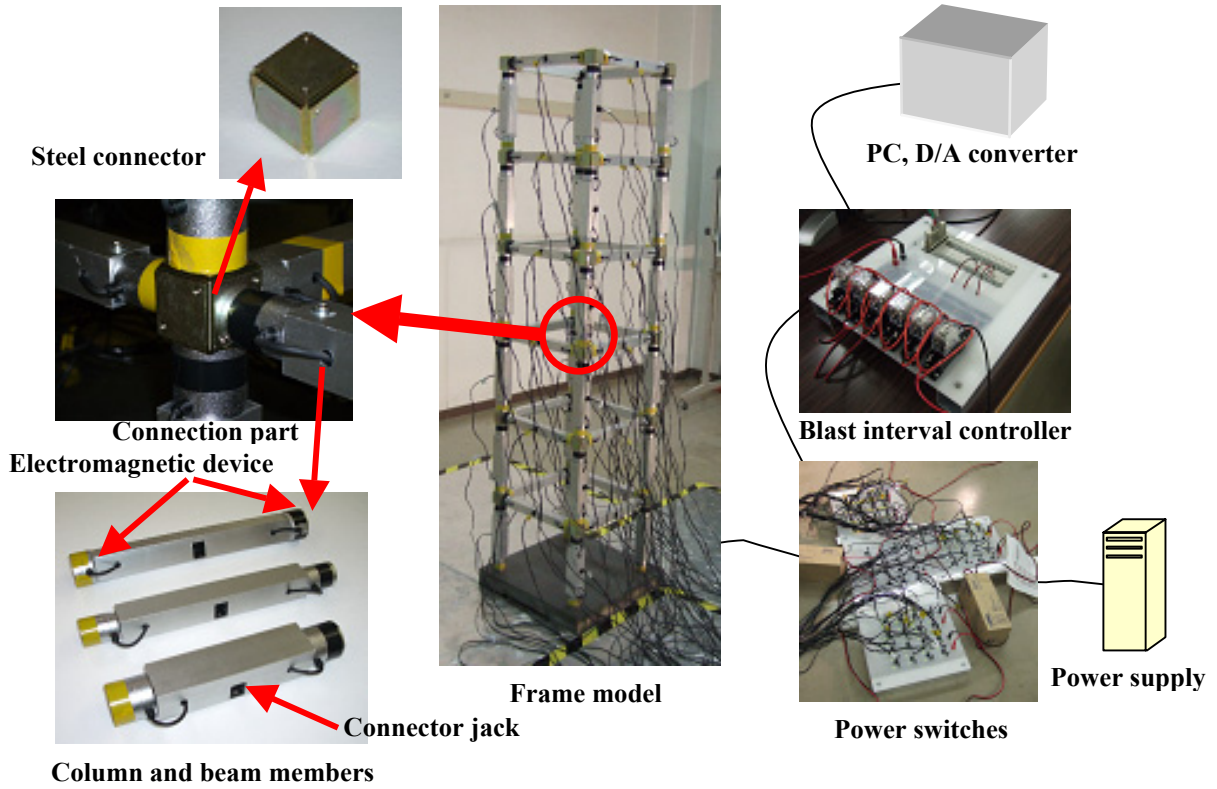


Figure 7: Outline of blast demolition experimental system

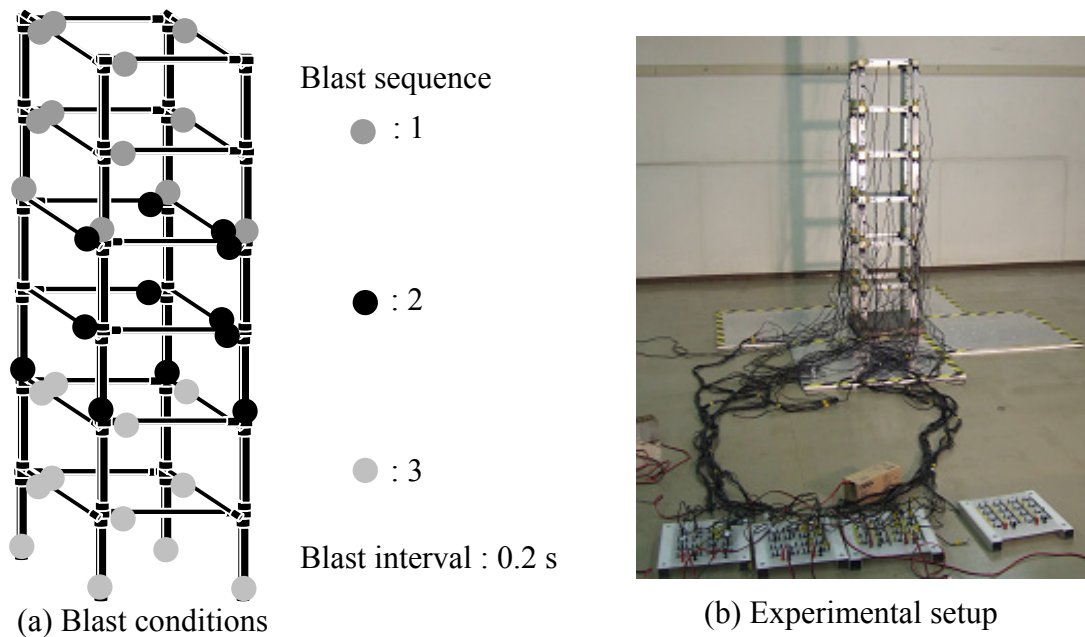
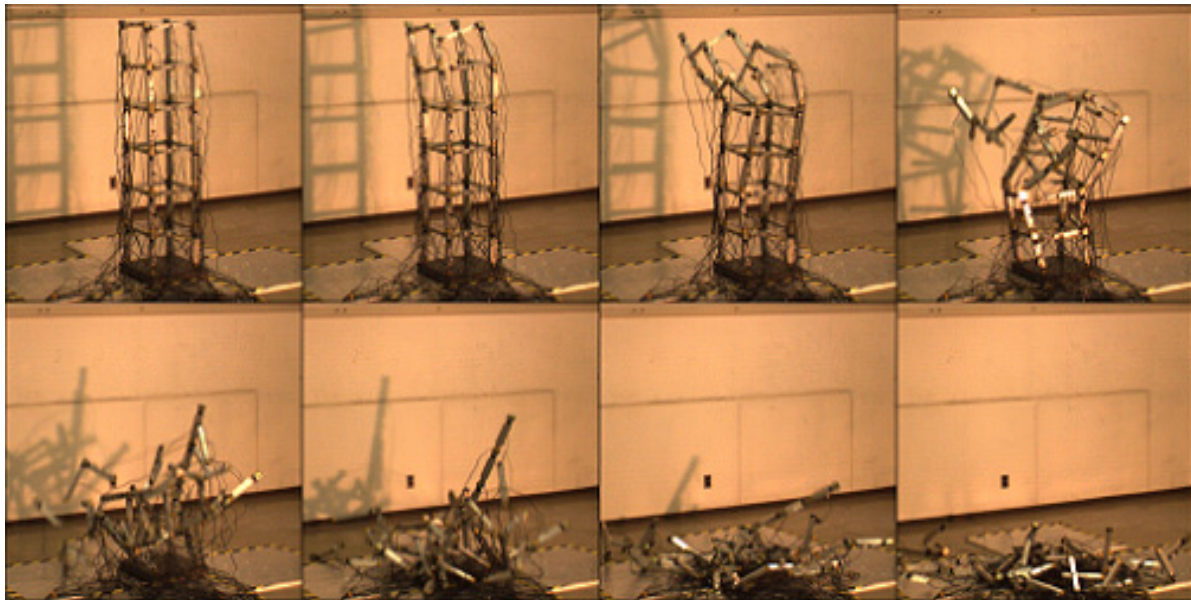
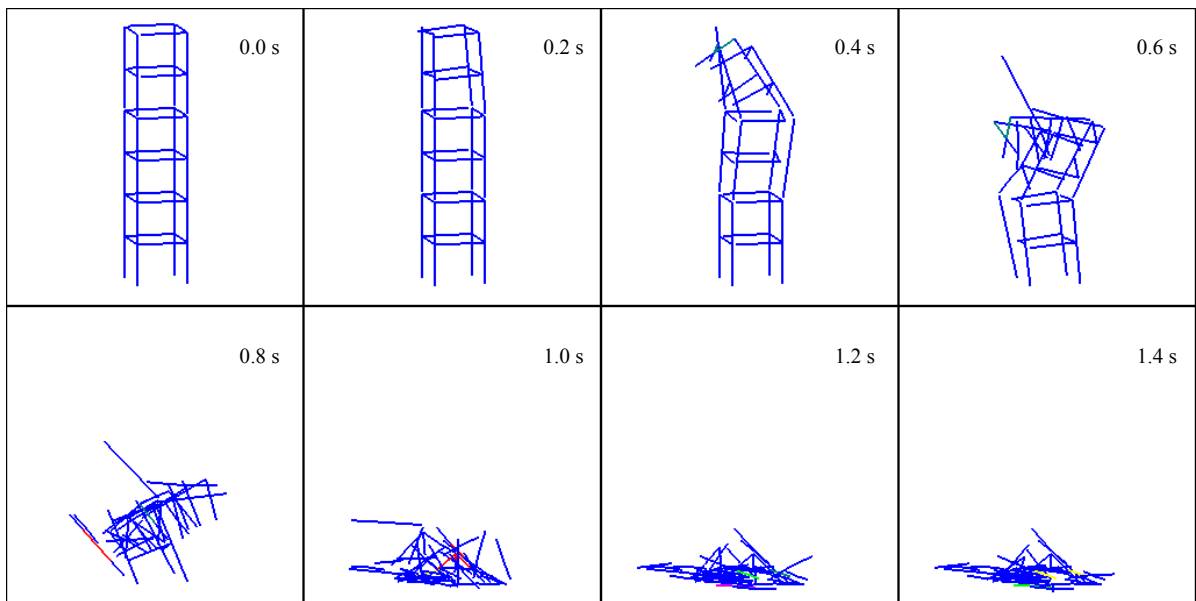


Figure 8: Blast conditions for a 6-story frame model





(a) Experimental result



(b) Numerical result

Figure 9: Comparison of demolition modes

A 6-story frame model is constructed using the developed devices. The blast conditions are shown in Fig. 8, where the blast points and the blast sequence are carefully selected to enable the floor sections to fold in one after another from the upper floors, to avoid fragments dispersing to a wider area. Figure 9 shows the comparison of demolition modes between the experimental and the numerical results. The interval between each frame is 0.2 s. The

expected mode is observed in either result, and both results are practically in good agreement with each other.

## CONCLUSIONS

In this paper, numerical and experimental approaches are taken to verify blast demolition problems. The ASI-Gauss technique is applied to numerical analyses, and the experimental system using electromagnetic devices is newly developed to compare the results quantitatively. Both results showed almost the same demolition mode, which indicates the validity of both the numerical code and the experimental system.

Some demolition experiments with a larger model are scheduled to verify the practicability and reliability of both approaches.

## ACKNOWLEDGMENTS

This work is partially supported by a Grant-in-Aid for Scientific Research, No.16206055, Japan Society for the Promotion of Science.

## REFERENCES

- Cundall, P.A. (1971). "A computer model for simulating progressive, large scale movement in blocky rock system." *Proc. of the International Symposium on Rock Mechanics*, II-8, 129-136.
- Isobe, D. and Lynn, K.M. (2004). "A Finite Element Code for Structural Collapse Analyses of Framed Structures under Impact Loads." *CD-ROM Proc. on 4th European Congress on Computational Methods in Applied Sciences and Engineering ECCOMAS 2004*, Jyvaskyla, Finland.
- Isobe, D. and Toi, Y. (2000). "Analysis of Structurally Discontinuous Reinforced Concrete Building Frames using the ASI Technique." *Computers & Structures*, 76, 471-481.
- Kinoshita, M., Hasegawa, A., Matsuoka, S. and Nakagawa, K. (1989). "An experimental study on explosive demolition methods of reinforced concrete building." *Proc. of the Japan Society of Civil Engineers*, 403(VI-10), 173-182.
- Ma, M.Y., Barbeau, P. and Penumadu, D. (1995). "Evaluation of active thrust on retaining walls using DDA." *J. of Computing in Civil Engineering*, 1, 820-827.
- Shi, G. H. and Goodman R. E. (1984). "Discontinuous deformation analysis." *Proc. of 25th U.S. Symposium on Rock Mechanics*, 269-277.
- Toi, Y. and Isobe, D. (1993). "Adaptively Shifted Integration Technique for Finite Element Collapse Analysis of Framed Structures." *Int. J. for Numerical Methods in Engineering*, 36, 2323-2339.
- Tosaka, N., Kasai, Y. and Honma, T. (1988). "Computer Simulation for Felling Patterns of Building." *Demolition Methods and Practice*, 395-403.
- Williams, G.T. (1990). "Explosive demolition of tall buildings in inner city areas." *Municipal Engineer*, 7(4), 163-173.
- Yarimer, E. (1989). "Demolition by Controlled Explosion as a Dynamical Process." *Structures under Shock and Impact*, 411-416.